# Dissociation and Recombination in the Photochemical Decay of Carbonyl Cyanide $CO(CN)_2$ in Cryogenic Matrixes

**H. U. Suter, R. Pfister, A. Furlan, and J. Robert Huber***

*Physikalisch-Chemisches Institut der Universität Zürich, Winterthurerstrasse 190, CH-8057 Zürich, Switzerland*

*Received: September 4, 2006; In Final Form: November 4, 2006*

The photochemistry of $CO(CN)_2$ in cryogenic matrixes has been investigated employing pulsed laser excitation at 193 nm. During irradiation, the parent molecule, the intermediate, and the final photoproducts were monitored by IR spectroscopy. Four new species were identified including the isocyano isomer of the parent NCC(O)-NC, cyanogen NCCN, isocyanogen CNCN, and CO according to spectroscopic features and ab initio calculations. After prolonged irradiation, the only remaining species were CO and the two isomers NCCN and CNCN. A reaction scheme is proposed which is in agreement with the first dissociation step being a branching of the decay path into the radical channel to CN + OCCN and the molecular channel to CO + $(CN)_2$. The caged radicals of the former reaction either recombine to the parent molecule and its isomer which are both photolyzed again or they react directly to the stable and final products.

## Introduction

Carbonyl cyanide $CO(CN)_2$ (Figure 1, insert) has attracted attention as a precursor for the OCCN radical and as a simple model system such as formaldehyde for the photoinduced decay into radical and molecular products.[1,2] Following photolysis of $CO(CN)_2$ in a molecular beam at 193 nm, the excited molecule was found to dissociate primarily (≈94%) via an α-cleavage to the radicals OCCN + CN. Under these conditions, only about 18% of the nascent OCCN fragments are unstable and decompose to CO + CN. The generation of a large fraction of stable OCCN radicals was thus directly demonstrated in this experiment which was carried out using a photofragment translational energy spectrometer combined with quadrupole mass detection.[1,2] Furthermore, the nascent CN fragments emerging from the α-cleavage and those from the spontaneous secondary decay of sufficiently hot COCN radicals were also probed by laser-induced fluorescence (LIF) and were discerned by their different translational and internal energy distributions.[3] A minor decay channel (≈6%) involves a concerted bond-breaking and bond-making process in a single kinetic step leading to the molecular products CO + $(CN)_2$.[2] In addition to the experimental work, the energy and the structure of the parent molecule, products, and transition-state species were calculated by ab initio methods to elucidate the complex photochemical decay.[4] In this context, it is interesting to note that photolysis of acetyl cyanide $CH_3$-COCN at 193 nm, which was expected to be an efficient source of OCCN radicals, showed no traces of this radical.[5,6]

Motivated by these results in the gas phase, we investigated $CO(CN)_2$ in cryogenic matrixes before, during, and after UV laser irradiation and probed the emerging photoproducts by infrared spectroscopy. The matrix environment is expected to trap and isolate intermediate species not accessible by spectroscopic means in the previous gas-phase experiments. The analysis of the spectra was carried out utilizing the results of ab initio calculations.

* Author to whom correspondence should be addressed. Tel.: 0041-44-6354461. Fax: 0041-44-6356838. E-mail: jrhuber@pci.unizh.ch.

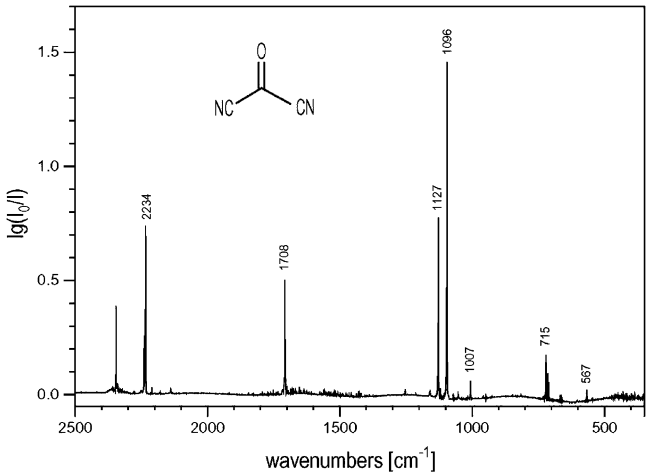


**Figure 1.** Infrared absorption spectrum of carbonyl cyanide $CO(CN)_2$ in an Ar matrix (dilution ratio 1:5000) at 12 K. Assignments are given in Table 1.

## Experimental Methods

The details of the apparatus and the method for matrix preparation have been presented elsewhere.[7] Briefly, the chamber was backfilled with a mixture of rare gas (Ar or Xe) and carbonyl cyanide in mole ratios of 1:1000−5000. Films of 55−600 μm were deposited on a cold CsI plate at a rate of ≈10−20 μm/min for 5−30 min. The deposition rate was estimated by comparison with previous IR interferometric measurements.[8]

IR spectra in the range 250−4000 $cm^{-1}$ were recorded using a Fourier transform infrared (FTIR) spectrometer (BIO-RAD FTS 175C) equipped with a closed-cycle low-temperature cryostat (Displex CS-202, Air Products). The cryostat is equipped with two CsI windows and a quartz window. The sample was irradiated through the quartz window with UV light at 193 nm using an ArF excimer laser (Lambda Physik EMG 101) at a fluence of ≈4 $mJ/cm^2$ (pulse duration ≈ 20 ns). After exposures to usually 100−5000 laser shots at 10 Hz, the substrate was rotated by 90° for the acquisition of an IR spectrum. Single spectra were obtained by averaging 100 times

10.1021/jp065731l CCC: $37.00 
Published on Web 01/12/2007

**TABLE 1: IR Frequencies and Relative Intensities of $CO(CN)_2$ in Ar and Xe Matrixes**

| Ar matrix | | Xe matrix | | gas phase | | |
|---|---|---|---|---|---|---|
| $cm^{-1}$ | int.[a] | $cm^{-1}$ | int.[a] | $cm^{-1}$ | int. | assignment[b] |
| 2240 | 0.25 | | | | | $\nu_1(a_1)$ CN stretch |
| 2234 | 1.00 | 2229 | 1.00 | 2230 | vs | $\nu_2(b_2)$ CN stretch |
| 1708 | 0.75 | 1701 | 0.80 | 1711 | vs | $\nu_3(a_1)$ CO stretch |
| 1127 | 0.90 | 1125 | 0.83 | 1124 | vs | $\nu_4(b_2)$ CC stretch with |
| 1096 | 1.55 | 1091 | 0.94 | 1102 | vs | $\nu_5(b_2)$ in Fermi resonance |
| 1007 | 0.10 | 1002 | 0.08 | 1004 | m | $\nu$ combination |
| 715 | 0.08 | 711 | 0.10 | 712 | s | $\nu_6(a_1/b_1)$ CC stretch |
| 567 | 0.05 | 560 | 0.04 | 553 | m | $\nu_7(a_1)$ CCC scissoring |

[a] Intensity integrated over peak area and normalized to $\nu_2$. Only peaks with a relative intensity of >0.04 are listed. [b] Assignments according to the present calculation and refs 16 and 21.

at a resolution of $\Delta\nu = 0.25$ $cm^{-1}$, whereas for the kinetic data 50 measurements were averaged at $\Delta\nu = 2$ $cm^{-1}$. The sample temperature was held at 12 K during the photolysis and the spectrometric measurements. Annealing of the fresh and the fully photolyzed samples was carried out at 35 K for the Ar matrix and 60 K for the Xe matrix.

The highly toxic carbonyl cyanide $CO(CN)_2$ was synthesized by reaction of tetracyanoethylene oxide with *n*-butyl sulfide at 50 °C.[9] The yellowish product with a boiling point of 66 °C was purified by four distillations at reduced pressure. The gas-phase UV absorption spectrum of $CO(CN)_2$ in the range of 190−410 nm was recorded previously and is displayed in Figure 1 of ref 2.

## Calculation Methods

The vibrational frequencies of the parent molecule and expected intermediate and product species were calculated with the harmonic force fields using the Gaussian03 program package[10] with the Becke3LYP density functional[11] together with the 6-31g** AO basis set. The choice of this type of calculation was given by our experience with previous calculations which showed a rather monotonic behavior for the scaling using the scaling factor of 0.963 for the calculated frequencies.[12] The normal coordinate analysis was performed by transforming the output of the Gaussian03 to the GAMESS Program.[13] The vibrational frequencies were further analyzed in terms of the total energy decomposition (TED) of Pulay and Tarok[14] (not shown).

## Results

**UV Spectrum of $CO(CN)_2$.** At its low-energy region, the gas-phase absorption spectrum[2,15] starts with a weak band system showing a maximum at about 330 nm. This band, belonging to the $S_0 \rightarrow S_1$ ($n\pi^*$) transition localized on the CO group, is structured and exhibits at least 10 evenly spaced vibronic bands between 270 and 400 nm. This progression with an initial spacing of 1230 $cm^{-1}$ was assigned to the C═O stretching vibration in the $S_1$ state. Each of these bands is further split into eight narrow peaks separated by ≈128 $cm^{-1}$. According to our calculation, they are due to the excited-state in-plane $\delta$(N−C−C−C−N) bending mode ($a_1$) whose corresponding ground state frequency[16] is 127 $cm^{-1}$.

Beside the $n\pi^*$ transition, a strong absorption starts at around 220 nm and extends to below 190 nm (the lower limit of our previous measurement).[2] Although a definitive assignment of this transition is lacking, it probably involves a Rydberg $^1$(n,-3s) state by analogy with other carbonyl compounds[17,18] or as later suggested a $\pi_{CN}\pi^*_{CO}$ state.[19] The present photolysis experiments were carried out at 193 nm, where the absorption

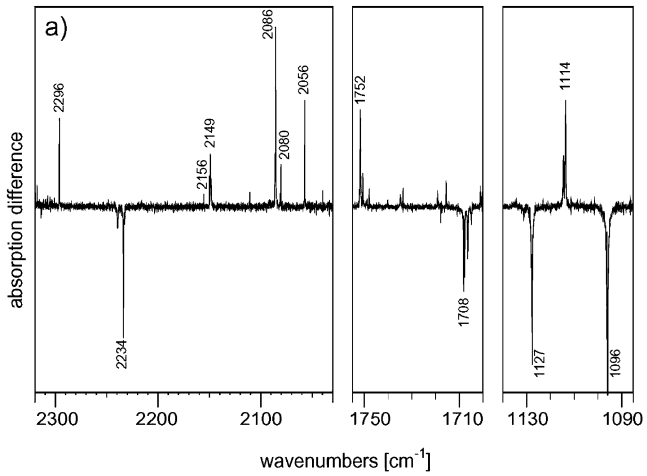


**Figure 2.** Photolysis of $CO(CN)_2$ in an Ar matrix (dilution ratio 1:5000) at 12 K. The difference IR absorption spectrum was recorded after 2000 laser pulses at 193 nm. The negative peaks indicate the disappearance of the reactant $CO(CN)_2$, and the positive peaks indicate the appearance of intermediate and final product species.

cross section $\epsilon$ is ≈2300 $dm^3$ $mol^{-1}$ $cm^{-1}$ ($\sigma = 8.7 \times 10^{-18}$ $cm^2$), about 1000 times greater than at the maximum of the $n\pi^*$ transition.

**Infrared Spectra of $CO(CN)_2$ and Its Photoproducts.** The IR spectrum of $CO(CN)_2$ in an Ar matrix shown in Figure 1 agrees well with the gas-phase spectrum previously reported[16,20] and later studied in detail by calculations.[21] Only a small matrix shift of a few wavenumbers and a splitting of some bands because of different site structures are the expected differences. Table 1 lists the results of the two studies. To aid the spectral analysis, IR spectra were also recorded in the "softer" Xe matrix where the vibrational frequencies are slightly red-shifted and the site splittings are different compared to the Ar matrix. A distinct difference is only observed in the intensity ratio of the two strong bands $\nu_3$ and $\nu_4$ which is in clear favor of $\nu_4$ in Ar and almost one in Xe. These two bands belong to a Fermi resonance involving a strong mixture between the fundamental, antisymmetric C−C stretch ($b_2$) at ≈1100 $cm^{-1}$ and the combination between the C−C−C bend ($a_1$, scissor) at around 560 $cm^{-1}$ and the C═O wag ($b_2$) according to a proposal by Miller et al.[16] Since the frequencies of these modes are different in the two matrixes, the degree of mixing changes as manifested by the band intensities. In the following discussion, we refer only to the frequencies in the Ar matrix.

Figure 2 shows a difference spectrum in the IR region between about 1000 and 2300 $cm^{-1}$ where only the sections with clearly discernible changes are displayed. They were recorded after 2000 laser shots at 193 nm. The disappearance of the $CO(CN)_2$ vibrational bands upon irradiation, indicated as negative amplitudes in the spectrum Figure 2, is accompanied

**TABLE 2: IR Frequencies and Relative Intensities of Intermediate Product Species**

| Ar matrix | | Xe matrix | | calculated | | |
|---|---|---|---|---|---|---|
| $cm^{-1}$ | int. | $cm^{-1}$ | int. | $cm^{-1}$ | int. | assignment[a] NC−(CO)−NC |
| 2086 | 1.0 | 2079 | 1.0 | 2088 | 1.0 | $\nu_2$ NC-isostretch |
| 2080 | 0.2 | 2074 | 0.1 | | | $\nu_2$ site structure |
| 1752 | 0.7 | 1747 | 0.5 | 1749 | 0.5 | $\nu_3$ CO stretch |
| 1114 | 0.9 | 1111 | 0.4 | 1105 | 0.7 | $\nu_4$ C−$C_o$−N stretch |
| 716 | 0.1 | | | 722 | <0.1 | $\nu_6$ |

[a] According to the calculation.

**TABLE 3: IR Frequencies of Final Products**

| Ar matrix $cm^{-1}$ | Xe matrix[a] $cm^{-1}$ | Ar matrix[b] $cm^{-1}$ | gas phase $cm^{-1}$ | assignment |
|---|---|---|---|---|
| 2296 | 2291 | 2294 | 2302[a] | CNCN |
| 2156 | 2152 | 2153 | 2158[c] | NCCN |
| 2149 | 2141 | 2150 | 2143[d] | CO |
| 2056 | 2052 | 2054 | 2060[a] | CNCN |

[a] Reference 30. [b] Reference 31. [c] Reference 28. [d] Reference 27.

by the appearance of at least nine new bands, the strongest and most distinct of which are listed in Tables 2 and 3. After prolonged excitation, only four distinct bands located in the region 2050−2300 $cm^{-1}$ survive (Figure 3a) suggesting that the bands at 2086, 2080, 1752, and 1114 $cm^{-1}$ as well as a weak band at 716 $cm^{-1}$ (not shown) belong to intermediate species. The frequencies of the final product bands are listed in Table 3.

The "kinetics" of the IR bands in terms of the growth and disappearance of the integrated peak intensities as a function of the number of laser shots shown in Figure 4 enabled us to discriminate among three product groups. While the $CO(CN)_2$ bands at 2234 and 1127 $cm^{-1}$ decrease steeply to 10% of their initial intensity after about 200 shots (Figure 4a, b), the intensity of the first group of product bands at 2086 and 1114 $cm^{-1}$, as well as that at 1752 $cm^{-1}$ (not shown), is zero before irradiation, reaches a maximum after 100−200 laser shots, and decreases thereafter to half of the maximum value within 1000 shots (Figure 4c, d). This behavior points to the creation and decay of an intermediate. Because interruption of the irradiation and subsequent annealing of the matrix does not change the intensities or frequencies of the three IR bands, we concluded that this intermediate species is stable in the cryogenic rare-gas environment and in the dark. It must possess a relatively high absorption cross section at 193 nm which promotes secondary photolysis as manifested by the consecutive reaction behavior. The second group of product peaks centered at 2296 and 2056 (Figure 4e, f) builds up slower than the first group. The band intensities reach the maximum after 800 shots followed by a slow decrease. Finally, the third group with peaks at 2156 and 2149 $cm^{-1}$ (Figure 4 g, h) approaches the maximum intensity after about 2000 laser shots which afterward remains constant. In separate experiments, we explored the initial growth of product bands after a restricted number of laser shots (about 30) for which the UV absorption of the parent molecule is not significantly changed. Immediately after the start of the laser, the growth rate rises without any delay and in monotonic fashion for the bands examined at 2086 and 1752 $cm^{-1}$ and those at 2149 and 2056 $cm^{-1}$.

Finally, Figure 4 provides only a qualitative picture of the evolution of the reactant and product concentrations. A quantitative analysis of the data was not feasible because of the lack of pertinent parameters such as the change of the UV absorption during extended irradiation and the extinction coefficients of the transient species. The intensities shown in Figure 4a−h are merely relative intensities; they are scaled to about the same height for each of the curves.

**TABLE 4: Calculated IR Spectrum of $CO(CN)_2$ and Comparison with Measurements in the Ar Matrix and in the Gas Phase (g)**

| species[a] | $cm^{-1}$ | int.[b] | $cm^{-1}$ (Ar) | $cm^{-1}$ (g)[c] |
|---|---|---|---|---|
| $\nu_1(a_1)$ | 2267 | 18 | 2240 | 2230 |
| $\nu_2(b_2)$ | 2264 | 89 | 2234 | 2230 |
| $\nu_3(a_1)$ | 1713 | 144 | 1708 | 1711 |
| $\nu_4(b_2)$ | 1093 | 239 | 1127[d] | 1124[d] |
| $\nu_5(b_2)$ | | | 1096[d] | 1102[d] |
| $\nu_6(b_1)$ | 728 | 7 | 715 | 712 |
| $\nu_7(a_1)$ | 706 | 4 | 708 | 712 |
| $\nu_8(a_1)$ | 567 | 4 | 567 | 553 |
| $\nu_9(b_2)$ | 536 | 1 | | 550 |
| $\nu_{10}(a_2)$ | 316 | 0 | | 307 |
| $\nu_{11}(b_2)$ | 242 | 13 | | 245 |
| $\nu_{12}(b_1)$ | 215 | 27 | | 208 |
| $\nu_{13}(a_1)$ | 124 | 5 | | 128 |

[a] $C_{2v}$ symmetry. [b] Intensity given in km/mol. [c] Reference 16. [d] Fermi resonance.

**Calculation of the IR Spectra of Feasible Intermediate Species.** Using ab initio methods, we calculated the IR spectra of the parent molecule given in Table 4 and potential intermediates created after photolysis of $CO(CN)_2$. According to experimental and theoretical results, we explored as intermediates the radicals OCCN and OCNC, both in their stable trans form, and the isomer of the parent molecule NC−C(O)−NC. The latter includes one cyanide group and one isocyanide group. Table 5 lists the predicted vibrational frequencies and their intensities for the two radicals, while Table 6 shows the corresponding spectral features for carbonyl(cyanide)(isocyanide). The stability and structure of the OCCN radical have been previously explored by ab initio calculation.[22]

## Discussion

**General Aspects.** The experimental results of the present study are summarized in Figures 1−4 and Tables 1−3. For the spectral analysis, we used ab initio calculations to predict the IR frequencies of pertinent vibrational bands of the parent molecule, potential intermediates, and product species as listed in Tables 4−6. Together with the results of the previous gas-phase investigations of the molecule in a cold beam,[1−3] we propose the following reaction scheme for the 193-nm photolysis of isolated $CO(CN)_2$ in an argon matrix cage.

$$NC{-}C(O){-}CN + h\nu \rightarrow NCCO + CN \quad (1)$$

$$\rightarrow CO + (CN)_2 \quad (2)$$

$$NCCO + CN \rightarrow NC{-}C(O){-}NC \quad (3a)$$

$$\rightarrow NC{-}C(O){-}CN \quad (3b)$$

$$\rightarrow CO + CN + CN \rightarrow CO + (CN)_2 \quad (4)$$

$$\rightarrow CO + (CN)_2 \quad (5)$$

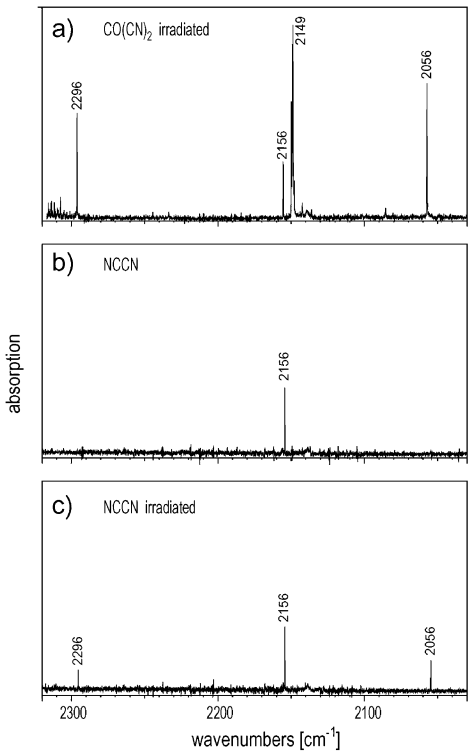


**Figure 3.** Infrared absorption spectra in Ar matrixes at 12 K of (a) the final products after extensive irradiation of $CO(CN)_2$, (b) NCCN (dilution ratio 1:1000), and (c) NCCN and the isomer CNCN after irradiation of the former at 193 nm.

According to the previous gas-phase work,[2] eqs 1 and 2 are the two initial dissociation steps with the radical decay (1) dominating the molecular decay (2). While in the gas phase, the two fragments of 1 escape each other, they are confined to a cage in the cold matrix where they are subject to competing decays. They can recombine (3a) and (3b), or the sufficiently hot NCCO radicals undergo secondary dissociation to CO and CN (4). In a second step, the latter react in the cage with the CN radical from the primary decay to form $(CN)_2$ (4). Finally, with eq 5 we consider the radical recombination which proceeds directly to the final products. Because of the continuous excitation, the products of steps 3a and 3b, which are the initial molecule and one of its isomers, are also photolyzed and the reaction sequence 1−5 starts over again. Equations 2, 4, and 5 are here the "exit channels" leading to the final products CO and $(CN)_2$ with their possible isomers.

**Intermediate Species.** In light of this reaction scheme, the results of our experiments and calculations are now discussed. The difference spectrum Figure 2 reveals eight new IR bands of which the ones at 2086, 2080, 1752, and 1114 $cm^{-1}$ show an intermediate behavior (Figure 4). Since OCCN and CN appear in the gas-phase photolysis,[2,3] we expected these bands to be associated with these species. The vibration of the CN radical in the gas phase is found at 2042 $cm^{-1}$ [23] with a small 0−1 transition moment, a factor 2.3 smaller than that of CO[24] (see below). Even when taking into account a few wavenumbers of matrix shift, no signal could be discerned in the region around 2042 $cm^{-1}$.

An experimental IR spectrum of OCCN is lacking. Our calculated spectra of the two possible structures of this radical, both in their stable trans forms (Table 5), are each dominated by two strong bands located at 2148 and 1896 $cm^{-1}$ and at 1982 and 1856 $cm^{-1}$, respectively. We found no transient IR bands nor final product bands within the uncertainty range of the calculation that could be assigned to the OCCN radical. Thus, we have to conclude that the two radicals CN and OCCN produced by the α-cleavage could not be isolated in appreciable concentration in the Ar matrix under our experimental conditions.

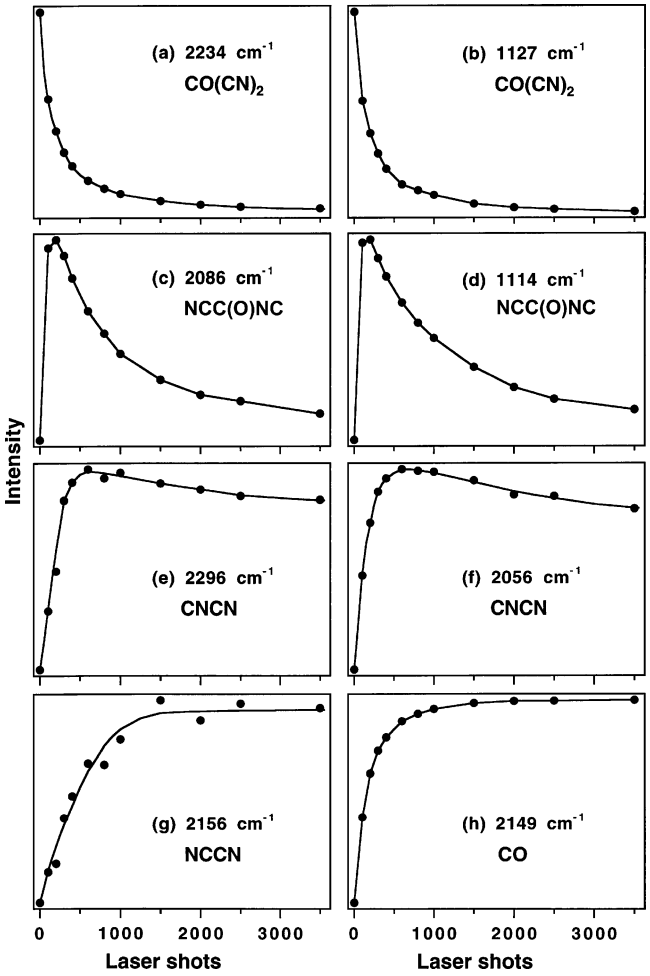


**Figure 4.** Photolysis of $CO(CN)_2$ in an Ar matrix (dilution ratio 1:5000) at 12 K. The integrated IR peak intensities as a function of the number of laser shots at 193 nm show the growth and disappearance of selected bands of reactant, intermediate, and products. The intensities represent relative intensities and are arbitrarily scaled to about the same height for each of the curves.

**TABLE 5: Calculated IR Spectra of Potential Intermediates**

| OC−CN | | | OC−NC | | |
|---|---|---|---|---|---|
| species[a] | $cm^{-1}$ | int. | species[a] | $cm^{-1}$ | int. |
| $\nu_1(a')$ | 2148 | 147 | $\nu_1(a')$ | 1982 | 216 |
| $\nu_2(a')$ | 1896 | 185 | $\nu_2(a')$ | 1856 | 231 |
| $\nu_3(a')$ | 794 | 5 | $\nu_3(a')$ | 877 | 28 |
| $\nu_4(a')$ | 544 | 2 | $\nu_4(a')$ | 575 | 6 |
| $\nu_5(a'')$ | 263 | 12 | $\nu_5(a')$ | 209 | 3 |
| $\nu_6(a')$ | 210 | 7 | $\nu_6(a'')$ | 182 | 2 |

[a] $\nu_1$ represents the C≡N stretch, $\nu_2$ the C═O stretch, and $\nu_3$ the C−C or C−N stretch.

Since cyanide molecules can isomerize to isocyanide molecules as has been demonstrated in argon matrixes for XCN compounds (X = H, F, Cl, Br, I),[25,26] we considered carbonyl(cyanide)(isocyanide), NCC(O)NC, a candidate for the intermediate. The calculated IR spectrum of this isomer (Table 6) reveals three strong vibrational bands at 2088 $cm^{-1}$ (CN-stretch), 1749 $cm^{-1}$ (CO-stretch), and 1105 $cm^{-1}$ (C−$C_o$−N stretch) and a weak one with still appreciable intensity at 722 $cm^{-1}$. A

**TABLE 6: Calculated IR Spectrum of the Potential Intermediate NC−(CO)−NC**

| species[a] | $cm^{-1}$ | int.[b] | $cm^{-1}$ (Ar) |
|---|---|---|---|
| $\nu_1(a')$ | 2273 | 39 | |
| $\nu_2(a')$ | 2088 | 483 | 2086 (1.2)[c] |
| $\nu_3(a')$ | 1749 | 213 | 1752 (0.7)[c] |
| $\nu_4(a')$ | 1105 | 337 | 1114 (0.9)[c] |
| $\nu_5(a')$ | 732 | 12 | |
| $\nu_6(a'')$ | 722 | 18 | 716 (0.1)[c] |
| $\nu_7(a')$ | 572 | 1 | |
| $\nu_8(a')$ | 528 | 7 | |
| $\nu_9(a'')$ | 280 | 12 | |
| $\nu_{10}(a')$ | 217 | 8 | |
| $\nu_{11}(a'')$ | 168 | 7 | |
| $\nu_{12}(a'')$ | 116 | 2 | |

[a] $C_s$ symmetry. [b] Intensity given in km/mol. [c] Relative intensities from Table 2.

comparison of these bands with the intermediate vibrational bands of the difference spectrum Figure 2 shows excellent agreement with respect to frequency and intensity (Table 2). Therefore, we assigned the intermediate spectrum to the isocyanide compound. This is a stable molecule, predicted by ab initio calculation to be about 75 kJ/mol higher in energy than carbonyl cyanide.[4] The remaining vibrational band at 2080 $cm^{-1}$ is probably caused by a matrix site structure slightly different from that of the strong 2086 $cm^{-1}$ band. The contribution of the corresponding site structure in the softer Xe matrix is much smaller (Table 2).

Having assigned the intermediate species, we consider its growth and decay during irradiation shown in Figure 4c and 4d. The initial transient accumulation of NCC(O)NC between 0 and 300 laser shots indicates the production rate of the intermediate to exceed initially its photodissociation rate. After prolonged irradiation, the repeated recombination reactions (3) die out by competition with the secondary dissociation or recombination discussed below and the intermediate disappears. Finally, we also calculated the IR spectrum of the di-isocyano isomer CNC(O)NC. However, no features of Figure 2 coincide with these calculated IR transitions.

**Final Photolysis Products.** The spectral features of the final products displayed in Figure 3a and listed in Table 3 are dominated by a vibrational transition at 2149 $cm^{-1}$. Since this is very close to the CO transition observed in the gas phase[27] at 2143 $cm^{-1}$, we concluded CO to be one of the final products. In the absence of an IR signal of trapped CN expected at 2042 $cm^{-1}$, the other three bands at 2056, 2156, and 2296 $cm^{-1}$ were supposed to arise from $(CN)_2$ which shows a growth curve (Figure 4) similar to CO. The molecule $(CN)_2$ is known to exist in two stable, well-investigated isomers:[28−34] cyanogen NCCN and isocyanogen CNCN, the latter being about 135 kJ/mol[2] (Hartree−Fock value $\approx$ 115 kJ/mol)[33] less stable than the former. To assign the final product bands in Figure 3a, we recorded the spectrum of a pure cyanogen sample in an Ar matrix over the pertinent region of 2000−2300 $cm^{-1}$. This spectrum is displayed in Figure 3b and exhibits a single band at 2156 $cm^{-1}$ which is in exact agreement with the smallest peak in Figure 3a. If this sample is subsequently subjected to irradiation at 193 nm, the molecule NCCN isomerizes partly to CNCN which becomes clearly evident in the spectrum of Figure 3c where two new bands appear at 2056 and 2296 $cm^{-1}$. The same IR bands were previously reported for CNCN in an Ar matrix[31] and, most important for the present study, they are present in Figure 3a which is the spectrum of the final photoproducts of $CO(CN)_2$. The IR peak due to NCCN at 2156 $cm^{-1}$ (Figure 3b and 3c) is only slightly decreased upon irradiation indicating that only a small fraction (<1%) of NCCN isomerizes to CNCN despite the two bands of the latter exhibiting a substantial absorption intensity. Even the most intense IR transitions of NCCN are known to be much weaker then those of CNCN. From gas-phase spectra, Stroh et al.[31] have determined an intensity ratio for $\nu_2$ (CNCN) to the $\nu_3$(NCCN) absorption (which in the matrix appear at 2056 and 2156 $cm^{-1}$, respectively) of 100:1. Adopting this result for the matrix spectrum of irradiated $CO(CN)_2$ in Figure 3a, we find a ratio $I(\nu_2):I(\nu_3) \approx 2.5$ which implies that the major final photolysis products are NCCN and CO and that only about 2.5% is CNCN relative to NCCN.

**Mechanism.** After determination of the intermediate NCC(O)NC and final products CO + NCCN and CNCN, we proceed to the mechanism of the photochemistry which is proposed to involve the reaction steps 1−5 introduced above. The primary dissociation routes (1) and (2) in the gas phase are expected to occur also in the matrix environment, and our experimental findings are consistent with this assumption. Decay route 1 creates the radicals OCCN and CN in a matrix cage. There they recombine to the parent molecule (3b) or to its isomer (3a). However, this process is in competition with the secondary dissociation of OCCN which emerges from the α-cleavage (1) with high vibrational excitation. In the gas phase, about 18% of these nascent radicals were found to possess sufficient internal energy to overcome the dissociation barrier[35] to CN + CO (4). In the matrix, these two radicals share a cage with the CN radical from the primary dissociation (1) and CN + CN react to $(CN)_2$. However, it is likely that eq 4 also proceeds in only one step, that is, OCCN + CN → CO + NCCN or CO + CNCN (5), without the prerequisite for a high vibrational energy content of OCCN and without dissociation prior to product formation. Both reactions (5) are strongly exothermic with $\Delta H = \approx -430$ kJ/mol and $\approx -295$ kJ/mol,[2,4] respectively, and are expected to proceed at most only over a small barrier as usually found for radical + radical reactions.

According to the scheme above, eqs 4 and 5 and the molecular dissociation (2) are the paths leading to the observed final photoproducts. On the basis of the gas-phase results, the efficiency of eq 4 is expected to be about 3 times that of eq 2. While eq 2 is probably not much influenced by the matrix, the yield of the spontaneous decay of hot OCCN (4) is probably lower in the matrix than in the gas phase because of vibrational energy transfer from the hot OCCN to the environment. The 18% in the gas phase thus represents merely an upper limit in the matrix. Should eq 5 be an efficient decay route for the OCCN radicals, the overall yield of eqs 4 and 5 to the final products could be substantial.

The continuous excitation conditions in our experiment causes the products of eq 3a and 3b to be also photolyzed, and the reaction sequence is repeated. Since the C−N bond in NCC(O)NC is weaker than the C−C bond in the parent molecule, α-cleavage is usually expected to favor the former. Therefore, the carbonyl(cyanide)(isocyanide) is assumed to preferentially dissociate along this weaker bond and the formation of the possible di-isocyano compound CNC(O)NC in eq 3a is unlikely which is consistent with our experiments and IR spectrum calculations. Besides CO, the final products are the two isomers NCCN and CNCN generated in a ratio of approximately 40:1. Their formation can occur by the sequential mechanism via OCCN + CN (4, 5) or by the concerted eq 2. The radical recombination is expected to yield to a large extent the thermodynamically favored product pair CO + NCCN but a small fraction may be created as CO + CNCN. It is also

conceivable that CNCN is formed by the molecular decay (2) when the isocyanide intermediate NCC(O)NC is photolyzed. A preference for the first or the second mechanism cannot be given. However, we believe to be able to exclude CNCN production via isomerization of NCCN in the photochemistry of $CO(CN)_2$ because the absorption cross section of NCCN at 193 nm ($\sigma = 9.6 \times 10^{-20}$ cm$^2$) is 2 orders of magnitude smaller than that of the parent molecule. The appearance rate of the IR signals at 2296 and 2056 cm$^{-1}$ (Figure 4) is already substantial when the absorption of $CO(CN)_2$ is still high and thus the shielding of NCCN from irradiation is essentially complete.

Finally, a direct photolysis of OCCN by the 193-nm radiation is considered unlikely and thus has not been included in the mechanism. Fast recombination reactions prevent the OCCN radical to reach an appreciable concentration relative to the parent molecule. The strong absorption of the latter at 193 nm shields OCCN (except maybe at the end of the prolonged photolysis) and protects it efficiently from photodissociation.

## Conclusion

In this study, our previous work on the photodissociation of $CO(CN)_2$ in a supersonic jet was extended to cryogenic matrixes. The parent molecule and its photoproduct in solid matrices were recorded upon irradiation by IR spectroscopy. In particular, we monitored growth and disappearance of the observed IR band intensities as a function of the number of laser pulses at 193 nm. The four new species NC(CO)NC, NCCN, CNCN, and CO were identified, whereas the major gas-phase fragments OCCN and CN turned out to be short-lived in the present matrix environment and hence could not be isolated. On the basis of ab initio calculations, the new bands appearing at 1114, 1752, and 2086 cm$^{-1}$ were assigned to NC(CO)NC, the isomer of the parent molecule. Upon further irradiation at 193 nm, the parent molecule as well as its isomer disappeared completely, while the stable products CO, cyanogen NCCN, and isocyanogen CNCN were formed. The two isomers showed a final ratio of about 40:1 while $CO:(CN)_2 = 1:1$. A reaction scheme of this photochemistry was proposed which is in agreement with the first dissociation step being a branching of the decay path into the radical channel (1) and the molecular channel (2). The caging of the nascent radicals CN and OCCN promotes recombination reactions among these radicals (3, 5) and among those from the decay of OCCN (4) which eventually yields the three final products.

**Acknowledgment.** This work was supported by the Swiss National Science Foundation. We thank Dr. Marco Nonella for program support and many helpful discussions.

## References and Notes

(1) Furlan, A.; Scheld, H. A.; Huber, J. R. *Chem. Phys. Lett.* **1998**, *282*, 1.
(2) Scheld, H. A.; Furlan, A.; Huber, J. R. *J. Chem. Phys.* **1999**, *111*, 923.
(3) Li, Q.; Carter, T.; Huber, J. R. *Chem. Phys. Lett.* **2000**, *323*, 105.
(4) Suter, H. U.; Huber, J. R.; Ha, T.-K. *Chem. Phys. Lett.* **1999**, *311*, 474.
(5) North, S. W.; Marr, A. J.; Furlan, A.; Hall, G. E. *J. Phys. Chem. A* **1997**, *101*, 9224.
(6) Furlan, A.; Scheld, H. A.; Huber, J. R. *J. Phys. Chem. A* **2000**, *104*, 1920.
(7) Müller, R. P.; Hollenstein, H.; Huber, J. R. *J. Mol. Spectrosc.* **1983**, *100*, 95.
(8) Müller, R. P.; Russegger, P.; Huber, J. R. *Chem. Phys.* **1982**, *70*, 281.
(9) Linn, W. J.; Webster, O. W.; Benson, R. E. *J. Am. Chem. Soc.* **1965**, *87*, 3651.
(10) Frisch, M. J.; Trucks, G. W.; Schlegel, H. B.; Scuseria, G. E.; Robb, M. A.; Cheeseman, J. R.; Montgomery Jr, J. A.; Vreven, T.; Kudin, K. N.; Burant, J. C.; Millam, J. M.; Iyengar, S. S.; Tomasi, J.; Barone, V.; Mennucci, B.; Cossi, M.; Scalmani, G.; Rega, N.; Petersson, G. A.; Nakatsuji, H.; Hada, M.; Ehara, M.; Toyota, K.; Fukuda, R.; Hasegawa, J.; Ishida, M.; Nakajima, T.; Honda, Y.; Kitao, O.; Nakai, H.; Klene, M.; Li, X.; Knox, J. E.; Hratchian, H. P.; Cross, J. B.; Adamo, C.; Jaramillo, J.; Gomperts, R.; Stratmann, R. E.; Yazyev, O.; Austin, A. J.; Cammi, R.; Pomelli, C.; Ochterski, J. W.; Ayala, P. Y.; Morokuma, K.; Voth, G. A.; Salvador, P.; Dannenberg, J. J.; Zakrzewski, V. G.; Dapprich, S.; Daniels, A. D.; Strain, M. C.; Farkas, O.; Malick, D. K.; Rabuck, D. D.; Raghavachari, K.; Foresman, J. B.; Ortiz, J. V.; Cui, Q.; Baboul, A. G.; Clifford, S.; Cioslowski, J.; Stefanov, B. B.; Liu, G.; Liashenko, A.; Piskorz, P.; Komaromi, I.; Martin, R. L.; Fox, D. J.; Keith, T.; Al-Laham, M. A.; Peng, C. Y.; Nanayakkara, A.; Challacombe, M.; Gill, P. M. W.; Johnson, B.; Chen, W; Wong, M. W.; Gonzalez, C.; and Pople, J. A. *Gaussian 03*, Revision C.02; Gaussian, Inc.: Wallingford, CT, 2004.
(11) Becke, A. D. *J. Chem. Phys.* **1993**, *98*, 5648.
(12) El-Azhary, A.-A.; Suter, H. U. *J. Phys. Chem. A* **1996**, *100*, 15056.
(13) Schmidt, M. W.; Baldridge, K. K.; Boatz, J. A.; Elbert, S. T.; Gordon, M. S.; Jensen, J. H.; Koseki, S.; Matsunaga, N.; Nguyen, K. A.; Su, S.; Windus, T. L.; Dupuis, M.; Montgomery, J. A. *J. Comput. Chem.* **1993**, *14*, 1347.
(14) Pulay, P.; Tarok, F. *Acta Chim. Acad. Sci. Hung.* **1966**, *47*, 273.
(15) Prochorow, J.; Tramer, A.; Wierzchowski, K. L. *J. Mol. Spectrosc.* **1966**, *19*, 45.
(16) Miller, F. A.; Harney, B. M.; Tyrell, J. *Spectrochim. Acta* **1971**, *27A*, 1003.
(17) Robin, M.B. *Higher Excited States of Polyatomic Molecules*; Academic: New York, 1975; Vol. 2.
(18) Gaines, G. A.; Donaldson, D. J.; Strickler, S. J.; Vaida, V. *J. Phys. Chem.* **1988**, *92*, 2762.
(19) Owrutsky, J. C.; Baronavski, A. P. *J. Chem. Phys.* **1999**, *110*, 11206.
(20) Bates, J. B.; Smith, W. H. *Spectrochim. Acta* **1970**, *26A*, 455.
(21) Tyrell, J. *Mol. Struct.* **1991**, *231*, 87.
(22) Francisco, J. S.; Liu, R. *J. Phys. Chem.* **1997**, *107*, 3840.
(23) Phillips, J. G. *Astrophys. J.* **1973**, *180*, 617.
(24) Treffers, R. R. *Astrophys. J.* **1975**, *196*, 883.
(25) Milligan, D. E.; Jacox, M. E. *J. Chem. Phys.* **1967**, *47*, 278.
(26) Fraenkel, R.; Haas, Y. *Chem. Phys. Lett.* **1993**, *214*, 235.
(27) Huber, K.P.; Herzberg, G. *Molecular Spectra and Molecular Structure IV. Constants of DiatomicMolecules*; Van Nostrand: New York, 1979.
(28) Jones, L. H. *J. Mol. Spectrosc.* **1973**, *45*, 55.
(29) North, S. W.; Hall, G. E. *J. Chem. Phys.* **1997**, *106*, 60.
(30) Stroh, F.; Winnewisser, M. *Chem. Phys. Lett.* **1989**, *155*, 21.
(31) Stroh, F.; Winnewisser, B. P.; Winnewisser, M.; Reisenauer, H. P.; Maier, G.; Goede, S. J.; Bickelhaupt, F. *Chem. Phys. Lett.* **1989**, *160*, 105.
(32) Nguyen, M. T. *Chem. Phys. Lett.* **1989**, *157*, 430.
(33) Sunil, K. K.; Yates, J. H.; Jordan, K. D. *Chem. Phys. Lett.* **1990**, *171*, 185.
(34) Hochlaf, M. *J. Mol. Spectrosc.* **2001**, *207*, 269.
(35) Horwitz, R. J.; Francisco, J. S.; Guest, J. A. *J. Phys. Chem.* **1997**, *101*, 1231.